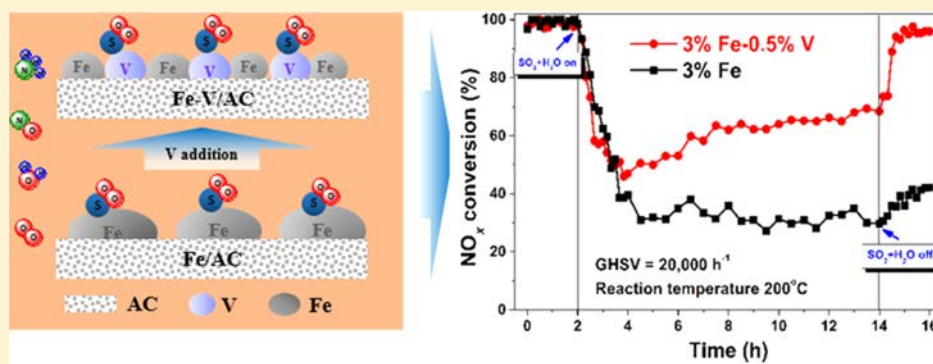# Effect of V_2O_5 Additive on the SO_2 Resistance of a Fe_2O_3/AC Catalyst for NH_3-SCR of NO_x at Low Temperatures

Weiwei Yang, Fudong Liu,*,[†] Lijuan Xie, Zhihua Lian,[‡] and Hong He*

Research Center for Eco-Environmental Sciences, Chinese Academy of Sciences 18 Shuangqing Road, Haidian District, Beijing 100085, P. R. China

S *Supporting Information*

ABSTRACT: The effect of vanadium oxide on an iron-based catalyst supported on activated carbon (AC) in the selective catalytic reduction of NOx by NH_3 (NH_3-SCR) was investigated in this work. A series of vanadium-modified Fe_2O_3/AC catalysts were prepared by a coimpregnation method. The addition of a small amount of vanadium oxide contributed to the higher dispersion of iron species on the surface of the catalyst. Among various vanadium-modified iron catalysts supported on AC, 3% Fe−0.5% V achieved the best SCR activity and SO_2 tolerance. In the presence of H_2O, SO_2 had a severe deactivation effect on both vanadium- and non-vanadium-modified catalysts, yet the inhibition effect of H_2O and SO_2 was reversible on 3% Fe−0.5% V at relatively low space velocity. It was found that the vanadium additive promoted the formation of sulfate species. The formed sulfate species increased the surface acidity and thus enhanced the tolerance toward SO_2.

1. INTRODUCTION

Nitrogen oxides (NO_x) from stationary sources contribute greatly to air pollution. Selective catalytic reduction (SCR) with NH_3 is an effective way to abate NO_x emissions and has been used throughout the world. Among numerous catalysts for NH_3-SCR, the V_2O_5/TiO_2 catalyst is found to be promising for practical application because of its high activity and good resistance to SO_2 poisoning in the desired temperature range.[1−8] However, the catalysts need to be operated above 350 °C to avoid deactivation by SO_2.[9] For power station boilers, a low-temperature process is desirable because it can avoid the need to reheat the flue gas and allows retrofitting of the SCR devices into existing systems.

Carbon materials as supports have received great attention in the NH_3-SCR field because of their high surface area and ease of modification. Vanadium oxide supported on activated carbon (AC) has been reported to show excellent NH_3-SCR activity in the presence of SO_2 above 180 °C when the V_2O_5 loading was less than 5%.[10,11] The catalyst was not deactivated but promoted instead by SO_2 significantly. It was proposed that vanadium oxide provided the adsorption and oxidation sites for SO_2, and the increased acidity due to surface sulfates enhanced the adsorption of NH_3, thus promoting the increase of SCR

activity.[12,13] In addition, the formed ammonium sulfate salts were more easily reduced by NO on AC possibly because of the better reducing ability of carbon, and hence their accumulation on the catalyst surface was avoided.[10,14−16] However, the V_2O_5/AC catalyst is not recommended for application in practice because of its limited activity at low temperatures.

Iron- and copper-based catalysts, especially iron and copper zeolite catalysts, have been studied widely because of their good SCR activity and high hydrothermal stability within a broad temperature window.[17−19] By comparison, copper zeolite shows higher NO_x conversion but lower N_2 selectivity, while iron zeolite has higher N_2 selectivity but modest NO_x conversion under standard SCR reaction conditions.[20] A lot of effort has been made to integrate the benefits of different catalysts (zeolite- and oxide-related catalysts) to achieve higher NO_x conversion over a wider temperature range.[6,7,21−23] It was reported that a Fe^{3+}−exchanged TiO_2−pillared clay catalyst showed higher SCR activity and N_2 selectivity than a

commercial V_2O_5–WO_3/TiO_2 catalyst.[22,24] Liu et al.[23,25] reported a novel and environmentally friendly iron titanate catalyst, prepared by a facile coprecipitation method, exhibiting excellent SCR activity and N_2 selectivity in the medium temperature range. Other iron oxide catalysts, such as γ-Fe_2O_3,[26,27] Mn–Fe spinel,[28] Fe–Mn,[29] Fe–Mn/Ti,[30,31] Fe–Ti spinel,[32] $Fe_2(SO_4)_3/TiO_2$,[33] and Fe–W/Zr,[34] have also been deeply investigated. However, the presence of SO_2 interfered severely with NO_x conversion over iron-related oxide catalysts below 300 °C.[20,22] Given the modest SCR activity of iron-based catalysts and superior SO_2 durability of vanadium-based catalysts, a catalyst combining the advantages of vanadium and iron species is a preferable alternative. Yang et al.[35] improved the SCR activity and SO_2 tolerance effectively by incorporating vanadium into Fe–Ti spinel. Liu et al.[36] developed a highly dispersed iron vanadate catalyst that demonstrated good SO_2 durability and high activity as well as N_2 selectivity in the medium temperature range.

A few bimetallic catalysts supported on carbon for NH_3-SCR have been reported.[37–39] García-Bordejé et al. found an improvement of the SCR activity by the addition of a second metal (iron, copper, manganese, and chromium) to vanadium supported on carbon-coated monolith catalysts.[38] Zhu et al. reported a series of V-M/AC (M = W, Mo, Zr, Sn) catalysts whose activities were promoted by SO_2 in the short term (except V–Mo/AC).[39] However, few studies involved iron-based catalysts supported on AC for NH_3-SCR.[40,41] In this work, we developed an Fe/AC catalyst modified by a small amount of V_2O_5, which achieved good activity as well as SO_2 durability at low temperatures. The influence of V_2O_5 on the SCR activity under SO_2-containing and SO_2-free conditions was elucidated in detail using relevant physical and chemical methods. It was found that modification by vanadium oxide increased the SO_2 durability of the catalyst because of its high acidity.

2. EXPERIMENTAL SECTION

2.1. Catalyst Preparation. The activated carbon (AC) support, before use, was ground to 40–60 mesh, followed by preoxidation with aqueous HNO_3 at 90 °C for 1.5 h. Then the samples were rinsed with distilled water to neutral pH and dried at 110 °C overnight.

Vanadium-modified iron catalysts supported on carbon were prepared by a coimpregnation method. Briefly, the pretreated carbon was impregnated with the required amount of iron nitrate and ammonium metavanadate in an oxalic acid solution. The mixture was evaporated using a rotary evaporator at 60 °C until excessive water was removed, and then the mixture was dried at 110 °C overnight and calcined at 500 °C for 5 h under a N_2 atmosphere. The catalysts are denoted as 3% Fe–x% V/AC, where x represents the mass ratio of V/AC.

2.2. Activity Measurement. A fixed-bed quartz-tube reactor was used to measure the steady-state SCR activity of the catalysts under the following conditions: 500 ppm of NO, 500 ppm of NH_3, 5% O_2, 100 ppm of SO_2 (when used), 2.5% H_2O (when used), N_2 balance, and a 250 mL min^{-1} total flow rate. The catalyst loads were ca. 0.25 and 0.38 g, corresponding to gas hourly space velocities (GHSV) of 30000 and 20000 h^{-1}, respectively. Water vapor was generated by passing N_2 through a heated water bath (50 °C) containing deionized water. The relative concentrations of the effluent gas, including NO, NH_3, NO_2, and N_2O, were continuously measured by a Fourier transform infrared (FTIR) gas analyzer (NEXUS 670-FTIR)

equipped with a gas cell with 0.2 dm^3 volume. The NO_x conversion and N_2 selectivity were calculated as follows:

$$NO_x \ \text{conversion} = \left(1 - \frac{[NO]_{out} + [NO_2]_{out}}{[NO]_{in} + [NO_2]_{in}}\right) \times 100\% \tag{1}$$

N_2 selectivity

$$= \frac{[NO]_{in} + [NH_3]_{in} - [NO_2]_{out} - 2[N_2O]_{out}}{[NO]_{in} + [NH_3]_{in}}$$

$$\times 100\% \tag{2}$$

2.3. Characterization. The surface areas and pore structures of the catalysts were analyzed by N_2 adsorption at 77 K in a Quantachrome Quadrasorb SI-MP system. Prior to tests, the samples were outgassed at 300 °C for 6 h. The specific surface areas were calculated using the Brunauer–Emmett–Teller (BET) method. Barrett–Joyner–Halenda (BJH) and t-plot methods were used to obtain the mesopore and micropore volumes, respectively. The results are shown in Table 2.

X-ray diffraction (XRD) with a Cu Kα (λ = 0.15406 nm) radiation source was applied to characterize the crystalline phases over the carbon-supported catalysts on a computerized PANalytical X'Pert Pro diffractometer system. The data of 2θ from 10 to 90° were collected at 4° min^{-1} with a step size of 0.02°.

Temperature-programmed desorption (TPD) experiments were carried out from 30 to 800 °C in a fixed-bed quartz reactor using 50 mg of the catalysts. A quadrupole mass spectrometer (Cirrus, MKS) was used to record the signals of NH_3 (m/z 17 for NH_3, m/z 16 for NH_2, and m/z 15 for NH) and SO_2 (m/z 64) online. Before analysis, the catalysts were pretreated at 200 °C for 1 h in a flow of argon (50 mL min^{-1}) and then cooled to 30 °C.

X-ray photoelectron spectroscopy (XPS) with Al Kα radiation (1486.7 eV) was used to analyze the atomic state of iron, vanadium, and sulfur species adsorbed on the surface of the catalysts (Axis Ultra, Kratos Analytical Ltd.). The C 1s peak at 284.6 eV was used as an internal standard for peak position measurement.

The surface morphology and elemental composition of the samples were studied by field-emission scanning electron microscopy (SEM; SU-8020) combined with an energy-dispersive X-ray attachment. Transmission electron microscopy (TEM) was performed on a JEM-2010 microscope operating at 200 kV with a supplied CCD camera (FastScan-F114).

Inductively coupled plasma (ICP) with a radial view of the plasma (OPTMIA 2000DV) was used to analyze the component contents of the catalysts. Before testing, all of the samples were calcined at 500 °C in a muffle furnace, then dissolved using nitric acid solution, and diluted with water to 100 mL. The blank has been revised during this process.

3. RESULTS AND DISCUSSION

3.1. NH₃-SCR Activity of the Catalysts. Figure 1 shows NO_x conversion over 3% Fe/AC modified with different amounts of V_2O_5 as a function of the temperature between 100 and 250 °C. It can be seen that the pristine Fe/AC catalyst without modification by V_2O_5 already possessed good activity, achieving 50% NO_x reduction at as low as 100 °C. After the addition of V_2O_5 at 0.3 and 0.5 wt %, the activity of the catalysts
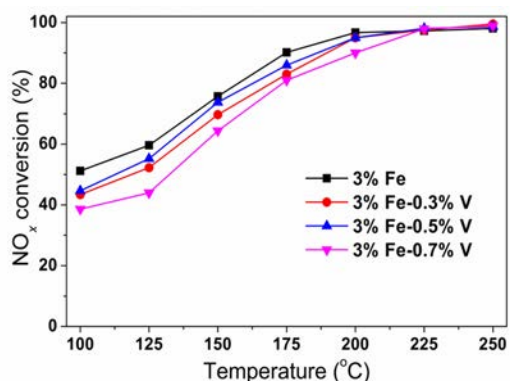
Figure 1. NH_3-SCR activity of a series of Fe−V/AC catalysts as a function of the temperature. Reaction conditions: 500 ppm of NO, 500 ppm of NH_3, 5% O_2, N_2 balance, and GHSV 30000 h^{-1}.

decreased by 5% at low temperatures but maintained the same activity as 3% Fe/AC above 200 °C; i.e., a small amount of vanadium additive did not influence the activity of the catalyst to a great extent. However, when the content of V_2O_5 was further increased to 0.7 wt %, the activity of the catalyst decreased remarkably. The results indicated that iron species may serve as dominant active sites. The decrease in the activity over vanadium-modified catalysts was possibly due to the covering of iron oxide by vanadium species.

In order to compare the SCR activity of the catalyst prepared in this study with the high-activity catalysts reported in the literature, the rate constants were calculated by eq 3, assuming a first-order reaction with respect to NO and diffusion-limitation-free:

$$k = -\frac{F_{NO}}{[NO]_{in} W} \ln(1 - X) \tag{3}$$

where F_{NO} is the molar NO feed rate, $[NO]_{in}$ is the molar NO concentration at the inlet (at the reaction temperature), W is the catalyst mass (g), and X is the NO_x conversion.

A comparison summary of the rate constants for the catalysts prepared in this study and those reported in the literature was made, as shown in Table 1. This comparison may not be persuasive because the reaction conditions tested for the catalysts were somehow different. Moreover, the support form

and the active component content vary over catalysts. For instance, for the high-activity manganese-based catalysts, the metal content was much higher than that of the catalyst prepared here.[8,28] However, the catalyst presented in this work shows higher activity than most other catalysts operating at low temperature, such as vanadium or iron catalysts supported on carbon-coated monoliths[40,42] and iron-based zeolite and oxide catalysts.[18,22,32] Given the low cost of AC, our catalyst in this study might be promising to be applied at low temperatures downstream of the desulfurizer and/or the particulate control device, although a better low-temperature activity needs to be developed further. Noting a high k value of Fe−V/AC at 250 °C, carbon gasification would take place at those high temperatures (above 250 °C), particularly with the doping of metals. One possible improvement can be alternation of the carbon support into monolithic form to reduce the power gasification, e.g., by coating carbon on cordierite monolith.[38]

3.2. Effect of the V_2O_5 Additive on the SO_2 and H_2O Tolerance of Catalysts. H_2O and SO_2 are important factors influencing the SCR activity over the catalysts. Figure 2 shows
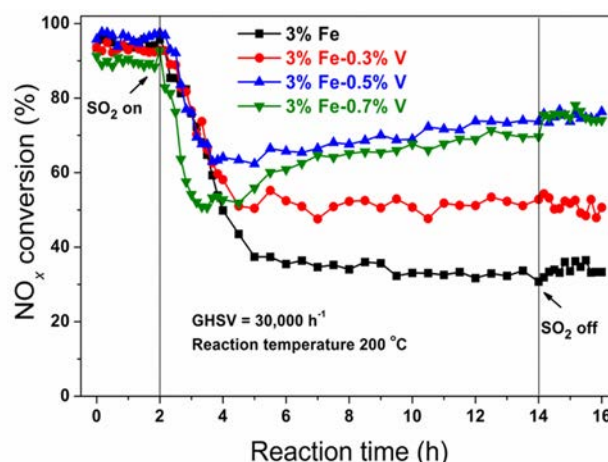

Figure 2. Effect of SO_2 on the SCR activity of Fe−V/AC serial catalysts as a function of time. Reaction conditions: 500 ppm of NO, 500 ppm of NH_3, 5% O_2, 100 ppm of SO_2 (when used), balance N_2, GHSV 30000 h^{-1}, and 200 °C.

Table 1. Performance of Various Catalysts for the SCR of NO with NH_3 at Low Temperature

catalyst	feed composition			T (°C)	X^e (%)	GHSV (h^{-1})	k (cm^3 g^{-1}s^{-1})	ref
	NO (ppm)	NH_3 (ppm)	O_2 (%)					
3% V/AC/C^a	700	800	3	150	72.1	17000	11.5	42
8% Fe/PFC^b	640	640	1	200	76.2	10000	11.39	40
5% V_2O_5/AC	500	560	3.3	250	79.7	90000	69.96	10
Fe-ZSM-5^c	500	500	5	150	6.7	320000	16.41	18
$(Fe_{2.5}Mn_{0.5})_{1-\delta}O_4$	500	500	2	150	90	150000	109	28
MnO_x−CeO_2	1000	1000	2	150	87	210000	120.66	8
5% V_2O_5/TiO_2^{d}	1000	1000	2	300	99.3	15000	13.17	1
7.5% Fe_2O_3 + 2.5% Cr_2O_3/TiO_2−PILC	1000	1000	2	200	42.6	60000	24.48	22
γ-Fe_2O_3	500	500	2	150	22.5	12000	12.8	32
3% Fe−0.5% V/AC	500	500	5	150	73.7	30000	31.59	this work
				250	98.5		122.8	

^{a}AC/C represents cordierite monoliths coated with mesoporous carbon derived from a polymer blend of poly(ethylene glycol) and furan resin. ^{b}Porous carbon prepared by phenol−formaldehyde resins from gasification, designated as PFC. ^{c}Fresh catalyst. ^{d}The feed contains 1000 ppm of SO_2 and 8% H_2O. ^{e}NO_x conversion and some data were read from the figures in the corresponding literature.

the effect of SO_2 on NO_x conversion of vanadium-modified Fe/ AC catalysts at 200 °C. All of these catalysts exhibited similar activity without SO_2 but decreased immediately upon the introduction of SO_2. The addition of different amounts of vanadium oxides improved the SO_2 durability of catalysts to different extents. When vanadium oxide loading increased from 0 to 0.5 wt %, the SCR activity of the catalysts rose accordingly in the presence of SO_2. However, the capability of SO_2 tolerance was no more enhanced when vanadium oxide was increased to 0.7 wt %.

As shown in Figure 1, the SCR reaction over these catalysts mainly occurred at iron sites. During the SCR reaction in the presence of SO_2, iron species may be converted into iron sulfate salts, leading to deactivation of the catalysts. It was reported that the oxidation of SO_2 to SO_3 was favored in the presence of vanadia.[43,44] H_2SO_4 formed through a combination of SO_3 and H_2O (produced by the SCR reaction) would migrate to the micropores of AC.[43] In this work, the addition of vanadia may increase the acidity of the catalysts because of the formation of more sulfuric acid on the surface of the catalysts and hence increase the activity of the catalysts. However, when the addition of V_2O_5 was increased to 0.7 wt %, excessive sulfuric acid would form and transfer to iron oxide, thus sulfurizing the active components, and the activity of the catalyst would not increase in this case. Clearly, among the various vanadium-modified catalysts, the 3% Fe−0.5% V catalyst exhibited the best variable-temperature SCR activity and SO_2 durability. Further investigation of this catalyst was conducted under relatively low space velocity.

To investigate the effect of H_2O on the SCR activity over 3% Fe and 3% Fe−0.5% V, NO_x conversion as a function of time at 200 °C was investigated, as shown in Figure 3. When H_2O was introduced individually into the feed, NO_x conversion over both 3% Fe and 3% Fe−0.5% V decreased to 85%, even though the vanadium-modified catalyst deactivated more slowly than the non-vanadium-modified catalyst. Upon removal of H_2O, NO_x conversion was reversed, indicating that the inhibition effect is due to the competitive adsorption of H_2O and NH_3 on acid sites.[45]

In the case of SO_2, 3% Fe showed severe deactivation, and NO_x conversion decreased to a steady-state value of 50%. For 3% Fe−0.5% V, NO_x conversion first decreased to 80% and then increased slowly to about 93%, suggesting that the vanadium additive enhanced the SO_2 tolerance of the catalyst. Figure S1 compares the SCR activities of 3% Fe and 3% Fe−0.5% V before and after sulfation as a function of the temperature. It was found that 0.5% V-modified 3% Fe catalyst shows a higher activity compared to 3% Fe, although both of these catalysts were severely SO_2-poisoned, especially at low temperatures.

When SO_2 and H_2O were present simultaneously, both 3% Fe and 3% Fe−0.5% V deactivated remarkably, indicating that H_2O accelerated deactivation of the catalysts. The NO_x reduction over 3% Fe dropped to 30% and then restored to 45% when SO_2 and H_2O were removed. In contrast, NO_x conversion over 3% Fe−0.5% V first decreased to 45%, then recovered slowly, and regained the initial value immediately when SO_2 and H_2O were cut off, which indicated that the inhibition effect of H_2O and SO_2 on vanadium-modified catalysts was reversible. This reversible effect of H_2O and SO_2 was also reported by García-Bordejé et al.,[46] who found that NO conversion over sulfated vanadia on carbon-coated monoliths regained the initial value when H_2O was shut off,
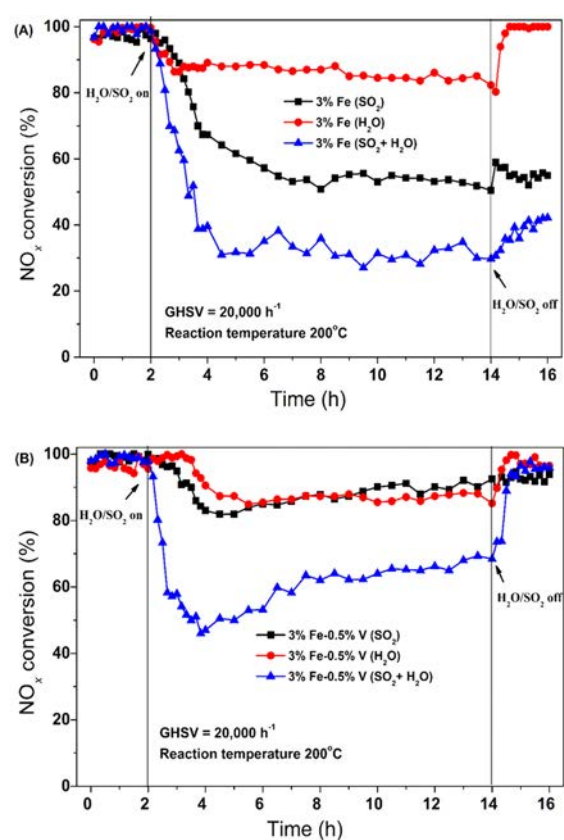

Figure 3. NH_3-SCR reactions over (A) 3% Fe and (B) 3% Fe−0.5% V/AC catalysts in the presence of 100 ppm of SO_2, 2.5 vol % H_2O, and 100 ppm of SO_2 + 2.5 vol % H_2O.

even though SO_2 was still in the gas flow at 200 °C. These results implied that addition of vanadia promoted the SO_2 and H_2O durability of catalysts. Detailed information regarding the mechanism will be discussed later.

3.3. BET. The surface area and pore structure distribution of raw AC, HNO_3-oxidized AC and Fe−V/AC catalysts are listed in Table 2. It can be seen that HNO_3 oxidation caused a great decrease in the BET area and micropore volume, possibly due to the blockage of the entrances to the micropores by oxygen functional groups as well as collapse of the pore structures.[47,48]

Table 2. Physical Properties of the Supports and Catalysts

catalyst	BET surface area ($m^2 g^{-1}$)	micropore volume ($cm^3 g^{-1}$)	micropore area ($m^2 g^{-1}$)	mesopore volume ($cm^3 g^{-1}$)
AC (raw)	839	0.370	762	0.103
AC (HNO_3)	665	0.283	600	0.083
3% Fe	871	0.396	780	0.280
3% Fe− 0.3% V	862	0.377	752	0.290
3% Fe− 0.5% V	1004	0.453	942	0.247
3% Fe− 0.7% V	1177	0.510	1073	0.302
3% Fe− 0.5% V[a]	953	0.418	809	0.349
3% Fe− 0.5% V[b]	674	0.303	601	0.219

[a]After reaction at 200 °C in the presence of SO_2 alone. [b]After reaction at 200 °C in the presence of SO_2 and H_2O, as shown in Figure 3.

After loading of the active components, the BET areas and micropore volumes increased, particularly for those catalysts modified by V_2O_5.

It was reported that micropores and mesopores are responsible for high NO conversion: micropores favor dispersion of the active component and mesopores guarantee accessibility of the reactants to the interior of AC.[12,47] In the present study, V_2O_5 addition led to new micropores and mesopores, thus contributing to the dispersion of Fe_2O_3 on the surface of AC. Even though the textural properties were improved by V_2O_5, the activity was not promoted, suggesting that the surface area was not the determining factor.

The physical properties of 3% Fe−0.5% V after SCR reaction in the presence of SO_2 and $SO_2 + H_2O$ are also listed in Table 2. Clearly, sulfation resulted in a dramatic decrease in the surface areas and micropore volumes, especially after treatment with SO_2 and H_2O. The results suggested that ammonium sulfate salts may have formed during the SCR reaction in the presence of $SO_2/SO_2 + H_2O$ and H_2O sped up the accumulation of ammonium sulfate salts on the surface of the catalysts and hence led to pore plugging.

3.4. XRD. XRD patterns of different catalysts are shown in Figure 4. All of the samples demonstrated two broad bands
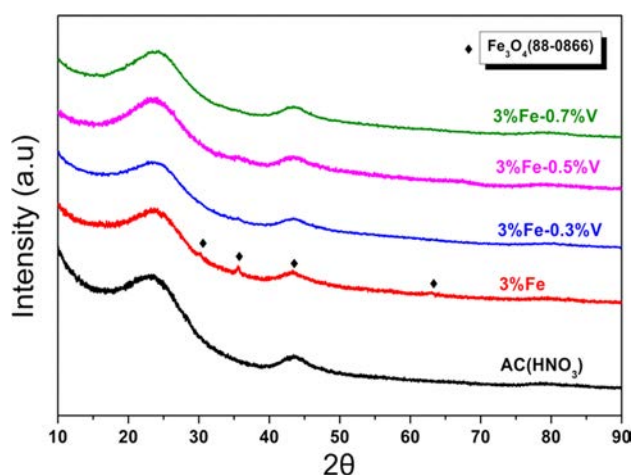

Figure 4. XRD profiles of the catalysts.

around 24° and 43°, corresponding to the amorphous carbon structure.[49] Compared to HNO_3-oxidized AC, weak diffraction peaks corresponding to the Fe_3O_4 phase were observed for the 3% Fe/AC catalyst. Because carbon materials can act as a reducing agent, the presence of Fe_3O_4 was possibly due to the reduction of some Fe_2O_3 by AC.[50] When a small amount of V_2O_5 was added to Fe/AC catalysts, the diffraction peaks of Fe_3O_4 disappeared, indicating that the V_2O_5 additive promoted the dispersion of iron oxide on the surface of AC.

Liu et al. found that Fe^{3+}−O−V^{5+} linkages formed on the surface of $FeVO_4/TiO_2$ catalysts and confirmed that an electronic inductive effect existed between Fe^{3+} and V^{5+} species by using XANES and XPS.[36] It was reported that the addition of V_2O_5 to a monolithic cordierite-based CuO/Al_2O_3 catalyst could significantly prevent CuO from aggregating and keep it active during the removal and regeneration processes.[51] In the present study, a small amount of vanadium might come in contact with iron to prevent iron oxide from aggregating, in accordance with the textural property results, as shown in Table 2.

3.5. TPD. To determine why vanadium additive increased the SO_2 and/or H_2O durability of the catalyst, TPD of SO_2 was performed over sulfated 3% Fe and 3% Fe−0.5% V catalysts (shown in Figure 5). The SO_2 desorption curves were fitted in the *Gaussian* program to differentiate sulfate species on the catalysts, with correlation coefficients (r^2) above 0.99. All of those desorption peaks could be deconvoluted into three groups of sub-bands centered at around 300, 330, and 400 °C. The peaks at around 300 and 330 °C were from decomposition of ammonium bisulfate, while the peak at around 400 °C was from decomposition of $Fe_2(SO_4)_3$.[52] It has been reported that decomposition of NH_4HSO_4 proceeds in two steps: the formation of NH_3 and H_2SO_4 starting at 170 °C and reduction of H_2SO_4 to SO_2 starting at 223 °C.[53] In this study, the decomposition temperatures of NH_4HSO_4 were higher than those reported, possibly because of the strong oxidation of SO_2 to H_2SO_4 by iron and vanadium oxides.[38,39]

In the presence of SO_2 and H_2O, more NH_4HSO_4 formed, suggesting that H_2O accelerated the deposition of NH_4HSO_4 regardless of the addition of vanadium oxide. As shown in Figure 5C,D, the addition of a small amount of vanadia resulted in the formation of a larger amount of sulfate species compared to the non-vanadium-doped catalyst (Figure 5A,B) and hence introduced extra Brønsted and Lewis acid sites (shown in Figure S2). The improved surface acidity was favorable for the adsorption of NH_3 and promoted the recovery of the SCR activity over 3% Fe−0.5% V when SO_2 and H_2O were cut off at lower space velocity, as shown in Figure 3.

3.6. XPS. To analyze the surface composition of 3% Fe and 3% Fe−0.5% V after SCR reaction in the presence of SO_2 and $SO_2 + H_2O$, as shown in Figure 3, XPS spectra were recorded (shown in Figure 6). The binding energies and surface atomic ratios are listed in Table 3. The binding energies of Fe 2p were around 710.0 eV in fresh and sulfated catalysts, indicating that iron had an oxidation state of Fe^{3+} (Figure 6A).[25,54,55] Compared to fresh catalysts (Figure 6B), a S 2p peak with a binding energy of 168.5 eV assigned to S^{6+} in the form of SO_4^{2-} appeared for 3% Fe and 3% Fe−0.5% V,[55,56] suggesting that sulfate species accumulated on the surface of the catalysts after treatment with SO_2 and $SO_2 + H_2O$. It was found that the vanadium additive promoted the accumulation of sulfate species on the surface of 3% Fe−0.5% V relative to 3% Fe, especially in the presence of $SO_2 + H_2O$, indicating that the presence of H_2O accelerated deposition of the sulfate species over vanadium-modified catalysts.

Table 3 shows that the Fe/C ratio decreased and the S/Fe ratio increased upon sulfation, which suggested that iron species were covered by sulfate species. The situation was more serious for the catalyst modified with vanadia because poor exposure of iron species was observed. These results confirmed that vanadia promoted the deposition of sulfate species. The Fe 2p and V 2p bands shifted slightly to higher binding energies in sulfated catalysts compared to those in fresh ones, which were due to the electron-withdrawing inductive effect by S=O covalent double bonds in sulfate in the vicinity of active sites. The obvious shift of Fe 2p to a higher binding energy after sulfation in the presence of H_2O over 3% Fe−0.5% V implied that more sulfate species attach around the iron species.

After sulfation in the presence of $SO_2 + H_2O$, the N/C ratio decreased; on the contrary, the S/N and S/Fe ratios increased, especially for 3% Fe−0.5% V. These results suggested that S^{6+} not only existed as NH_4HSO_4 and $Fe_2(SO_4)_3$ but also existed in another form. It was reported that H_2O could accelerate the
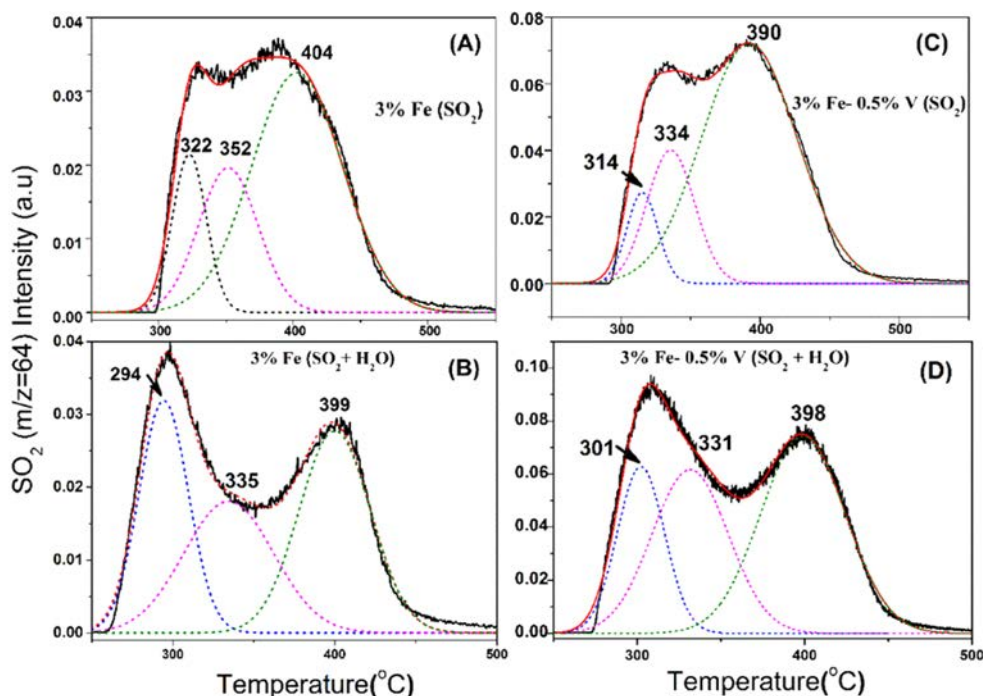
Figure 5. TPD of SO_2 from sulfate species formed on 3% Fe and 3% Fe−0.5% V at 200 °C for 12 h in the presence of SO_2 (A and C) and in the presence of $SO_2 + H_2O$ (B and D).

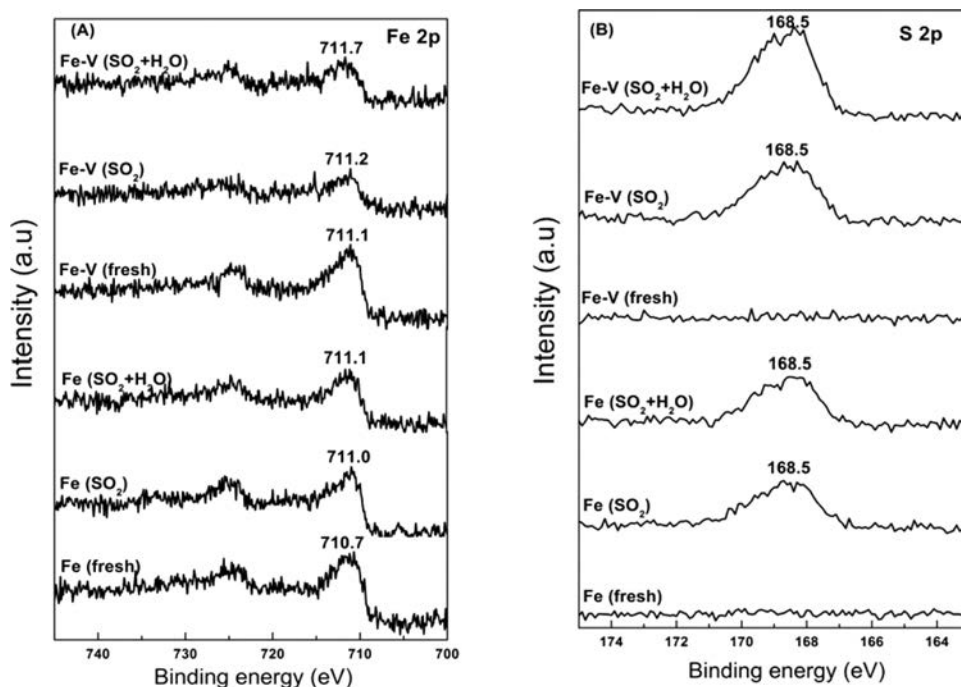**Figure 6.** XPS spectra of 3% Fe and 3% Fe−0.5% V after SCR reactions in the presence of SO_2 and $SO_2 + H_2O$: (A) Fe 2p; (B) S 2p.

formation of H_2SO_4, which tended to migrate into micropores.[45] Thus, sulfate species may exist in three forms after sulfation in the presence of $SO_2 + H_2O$, i.e., H_2SO_4, NH_4HSO_4, and $Fe_2(SO_4)_3$. The improvement in the surface acidity by those sulfate species may lead to enhanced SCR activity and the recovery of activity after treatment with $SO_2/SO_2 + H_2O$.

3.7. SEM and EDS Analysis. Figure 7 shows the SEM images and EDS analysis of 3% Fe-0.5% V after SCR reactions under different conditions. The active components, i.e., iron

oxide, distributed uniformly on the surface of AC. This fact was further confirmed by TEM, and the particle size of iron oxide was around 15−20 nm (Figure S3). Table 4 shows that the S and O content increased while the C content decreased after SCR reaction in the presence of SO_2 and SO_2+H_2O. The results further proved that sulfation led to accumulation of sulfate species on the surface of catalysts.

According to the TPD, XPS, and SEM results, reversible inhibition for SO_2 over the 3% Fe−0.5% V/AC catalyst was

Table 3. Binding Energies (eV) and Surface Atomic Ratios of 3% Fe and 3% Fe−0.5% V after SCR Reaction in the Presence of SO$_2$ or SO$_2$ + NH$_3$

catalyst	Fe 2p	V 2p	S 2p	Fe/C atom	N/C atom	S/Fe atom	S/N atom
Fe (fresh)	710.70			0.0077	0.006		
Fe (SO$_2$)	711.00		168.50	0.0057	0.023	0.54	0.14
Fe (SO$_2$ + H$_2$O)	711.10		168.50	0.0053	0.019	0.57	0.16
Fe−V (fresh)	711.10	516.70		0.0065	0.005		
Fe−V (SO$_2$)	711.20	517.10	168.50	0.0041	0.028	0.92	0.14
Fe−V (SO$_2$ + H$_2$O)	711.70	517.10	168.50	0.0042	0.025	1.16	0.20
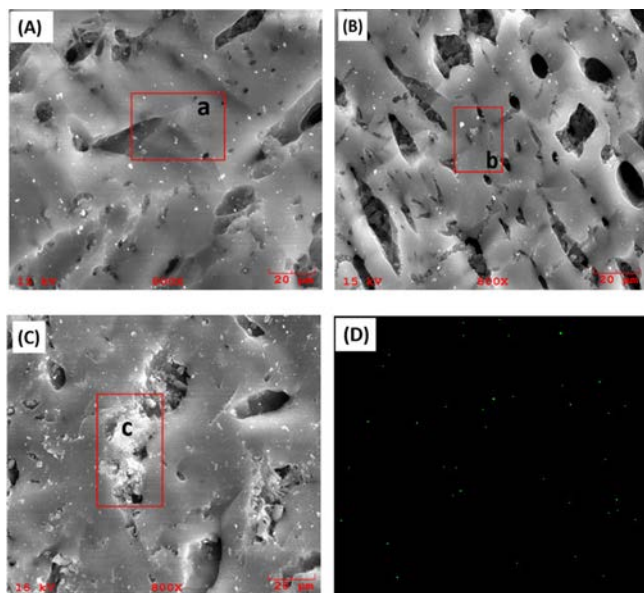
Figure 7. SEM images of 3% Fe−0.5% V: (A) fresh; (B) after sulfation in the presence of SO$_2$; (C) in the presence of SO$_2$ + H$_2$O. (D) EDS map for iron on fresh 3% Fe−0.5%V.

Table 4. EDS Analysis of 3% Fe−0.5% V under Employed Conditions

section	elements (atomic concentration %)				
	C	O	S	V	Fe
a	91.12	8.23	0.026	0.13	0.48
b	89.49	9.16	0.77	0.12	0.45
c	84.72	11.88	1.27	0.17	0.54

attributed to the introduction of trace vanadium oxide. Although the catalyst was poisoned by SO$_2$ to some extent because of the formation of a certain amount of iron sulfate, the promotion effect by vanadium was more pronounced by promoting the formation of ammonium bisulfate and sulfuric acid. The formed ammonium bisulfate and sulfuric acid can increase the surface acidity and then the adsorption of NH$_3$, which is a key step for enhancing the SCR activity.[11,38] Thus, the initial NO$_x$ conversion was regained when SO$_2$ (and H$_2$O) was (were) removed.

4. CONCLUSIONS

A series of trace vanadium oxide modified Fe/AC catalysts were prepared by a coimpregnation method. The addition of vanadium oxide contributed to the dispersion of iron on the carbon surface and increased the durability of the catalyst toward SO$_2$. However, no increase in tolerance toward SO$_2$ was observed when more vanadium oxide was added. 3% Fe−0.5%

V performed best, integrating the SCR activity and SO$_2$ tolerance, among various vanadium-modified iron catalysts supported on AC. The inhibition effect of H$_2$O and SO$_2$ on 3% Fe−0.5% V was reversible at relatively low space velocity based on the enhanced surface acidity, which was attributed to the deposition of large amounts of sulfate species by the introduction of a small amount of vanadium oxide. A combination of iron and vanadium species supported on AC may be a promising catalyst for NO$_x$ removal at low temperatures for stationary sources although carbon gasification needs to be considered further.

■ ASSOCIATED CONTENT

Ⓢ Supporting Information

The Supporting Information is available free of charge on the ACS Publications website at DOI: 10.1021/acs.iecr.5b04974.

ICP-OES of catalysts, NH$_3$-SCR activity over 3% Fe/AC and 3% Fe−0.5% V/AC catalysts before and after sulfation by 100 ppm of SO$_2$, NH$_3$-TPD patterns for fresh and sulfated 3% Fe and 3% Fe−0.5% V, and TEM images of 3% Fe−0.5% V catalyst (PDF)

■ AUTHOR INFORMATION

Corresponding Authors
*E-mail: lfd1982@gmail.com (F.L.).
*E-mail: honghe@rcees.ac.cn (H.H.). Tel: +86 10 62849123. Fax: +86 10 62849123.

Present Addresses
†F.L.: BASF Corp., 25 Middlesex/Essex Turnpike, Iselin, NJ 08830.
‡Z.L.: Institute of Urban Environment, Chinese Academy of Sciences, 1799 Jimei Road, Xiamen 361021, China.

Notes
The authors declare no competing financial interest.

■ ACKNOWLEDGMENTS

■ REFERENCES

(1) Chen, J. P.; Yang, R. T. Role of WO$_3$ in Mixed V$_2$O$_5$-WO$_3$-TiO$_2$ Catalysts for Selective Catalytic Reduction of Nitric Oxide with Ammonia. *Appl. Catal., A* **1992**, *80*, 135.

(2) Liu, K.; Liu, F.; Xie, L.; Shan, W.; He, H. DRIFTS Study of a Ce−W Mixed Oxide Catalyst for the Selective Catalytic Reduction of NOx with NH$_3$. *Catal. Sci. Technol.* **2015**, *5*, 2290.

(3) Zhang, D.; Zhang, L.; Fang, C.; Gao, R.; Qian, Y.; Shi, L.; Zhang, J. MnOx−CeOx/CNTs Pyridine-Thermally Prepared via a Novel in Situ Deposition Strategy for Selective Catalytic Reduction of NO with NH$_3$. *RSC Adv.* **2013**, *3*, 8811.

(4) Xiong, S.; Xiao, X.; Liao, Y.; Dang, H.; Shan, W.; Yang, S. Global Kinetic Study of NO Reduction by NH_3 over V_2O_5–WO_3/TiO_2: Relationship between the SCR Performance and the Key Factors. *Ind. Eng. Chem. Res.* **2015**, *54*, 11011.

(5) Shan, W.; Liu, F.; He, H.; Shi, X.; Zhang, C. An Environmentally-Benign CeO_2-TiO_2 Catalyst for the Selective Catalytic Reduction of NOx with NH_3 in Simulated Diesel Exhaust. *Catal. Today* **2012**, *184*, 160.

(6) Shan, W.; Liu, F.; He, H.; Shi, X.; Zhang, C. A Superior Ce-W-Ti Mixed Oxide Catalyst for the Selective Catalytic Reduction of NOx with NH_3. *Appl. Catal., B* **2012**, *115−116*, 100.

(7) Lian, Z.; Liu, F.; He, H. Enhanced Activity of Ti-Modified V_2O_5/ CeO_2 Catalyst for the Selective Catalytic Reduction of NOx with NH_3. *Ind. Eng. Chem. Res.* **2014**, *53*, 19506.

(8) Qi, G.; Yang, R. T. Performance and Kinetics Study for Low-Temperature SCR of NO with NH3 over MnOx−CeO_2 Catalyst. *J. Catal.* **2003**, *217*, 434.

(9) Busca, G.; Lietti, L.; Ramis, G.; Francesco, B. Chemical and Mechanistic Aspects of the Selective Catalytic Reduction of NOx by Ammonia over Oxide Catalysts. *Appl. Catal., B* **1998**, *18*, 1.

(10) Zhu, Z.; Liu, Z.; Niu, H.; Liu, S. Promoting Effect of SO_2 on Activated Carbon-Supported Vanadia Catalyst for NO Reduction by NH_3 at Low Temperatures. *J. Catal.* **1999**, *187*, 245.

(11) Hou, Y.; Huang, Z.; Guo, S. Effect of SO_2 on V_2O_5/ACF Catalysts for NO Reduction with NH_3 at Low Temperature. *Catal. Commun.* **2009**, *10*, 1538.

(12) Li, P.; Liu, Q.; Liu, Z. N_2O and CO_2 Formation during Selective Catalytic Reduction of NO with NH_3 over V_2O_5/AC Catalyst. *Ind. Eng. Chem. Res.* **2011**, *50*, 1906.

(13) Li, P.; Liu, Z.; Li, Q.; Wu, W.; Liu, Q. Multiple Roles of SO_2 in Selective Catalytic Reduction of NO by NH_3 over V_2O_5/AC Catalyst. *Ind. Eng. Chem. Res.* **2014**, *53*, 7910.

(14) Zhu, Z.; Niu, H.; Liu, Z.; Liu, S. Decomposition and Reactivity of NH_4HSO_4 on V_2O_5/AC Catalysts Used for NO Reduction with Ammonia. *J. Catal.* **2000**, *195*, 268.

(15) Zhu, Z.; Liu, Z.; Niu, H.; Liu, S.; Hu, T.; Liu, T.; Xie, Y. Mechanism of SO_2 Promotion for NO Reduction with NH_3 over Activated Carbon-Supported Vanadium Oxide Catalyst. *J. Catal.* **2001**, *197*, 6.

(16) Huang, Z.; Zhu, Z.; Liu, Z.; Liu, Q. Formation and Reaction of Ammonium Sulfate Salts on V_2O_5/AC Catalyst during Selective Catalytic Reduction of Nitric Oxide by Ammonia at Low Temperatures. *J. Catal.* **2003**, *214*, 213.

(17) Shwan, S.; Nedyalkova, R.; Jansson, J.; Korsgren, J.; Olsson, L.; Skoglundh, M. Hydrothermal Stability of Fe−BEA as an NH3-SCR Catalyst. *Ind. Eng. Chem. Res.* **2012**, *51*, 12762.

(18) Shi, X.; Liu, F.; Xie, L.; Shan, W.; He, H. NH_3-SCR Performance of Fresh and Hydrothermally Aged Fe-ZSM-5 in Standard and Fast Selective Catalytic Reduction Reactions. *Environ. Sci. Technol.* **2013**, *47*, 3293.

(19) Xie, L.; Liu, F.; Ren, L.; Shi, X.; Xiao, F. S.; He, H. Excellent Performance of One-Pot Synthesized Cu-SSZ-13 Catalyst for the Selective Catalytic Reduction of NOx with NH_3. *Environ. Sci. Technol.* **2014**, *48*, 566.

(20) Metkar, P. S.; Harold, M. P.; Balakotaiah, V. Selective Catalytic Reduction of NOx on Combined Fe- and Cu-Zeolite Monolithic Catalysts: Sequential and Dual Layer Configurations. *Appl. Catal., B* **2012**, *111−112*, 67.

(21) Shakya, B. M.; Harold, M. P.; Balakotaiah, V. Simulations and Optimization of Combined Fe- and Cu-Zeolite SCR Monolith catalysts. *Chem. Eng. J.* **2015**, *278*, 374.

(22) Cheng, L. S.; Yang, R. T.; Chen, N. Iron Oxide and Chromia Supported on Titania-Pillared Clay for Selective Catalytic Reduction of Nitric Oxide with Ammonia. *J. Catal.* **1996**, *164*, 70.

(23) Liu, F.; He, H.; Zhang, C. Novel Iron Titanate Catalyst for the Selective Catalytic Reduction of NO with NH_3 in the Medium Temperature Range. *Chem. Commun.* **2008**, 2043.

(24) Long, R. Q.; Yang, R. T. Selective Catalytic Reduction of Nitrogen Oxides by Ammonia over Fe^{3+}-Exchanged TiO_2-Pillared Clay Catalysts. *J. Catal.* **1999**, *186*, 254.

(25) Liu, F.; He, H. Structure-Activity Relationship of Iron Titanate Catalysts in the Selective Catalytic Reduction of NOx with NH_3. *J. Phys. Chem. C* **2010**, *114*, 16929.

(26) Mou, X.; Zhang, B.; Li, Y.; Yao, L.; Wei, X.; Su, D. S.; Shen, W. Rod-shaped Fe_2O_3 as an Efficient Catalyst for the Selective Reduction of Nitrogen Oxide by Ammonia. *Angew. Chem., Int. Ed.* **2012**, *51*, 2989.

(27) Liu, C.; Yang, S.; Ma, L.; Peng, Y.; Hamidreza, A.; Chang, H.; Li, J. Comparison on the Performance of α-Fe2O3 and γ-Fe_2O_3 for Selective Catalytic Reduction of Nitrogen Oxides with Ammonia. *Catal. Lett.* **2013**, *143*, 697.

(28) Yang, S.; Wang, C.; Li, J.; Yan, N.; Ma, L.; Chang, H. Low Temperature Selective Catalytic Reduction of NO with NH_3 over Mn−Fe Spinel: Performance, Mechanism and Kinetic study. *Appl. Catal., B* **2011**, *110*, 71.

(29) Long, R. Q.; Yang, R. T.; Chang, R. Low Temperature Selective Catalytic Reduction (SCR) of NO with NH3 over Fe-Mn Based Catalysts. *Chem. Commun.* **2002**, 452.

(30) Jiang, B. Q.; Wu, Z. B.; Liu, Y.; Lee, S. C.; Ho, W. K. DRIFT Study of the SO_2 Effect on Low-Temperature SCR Reaction over Fe-Mn/TiO_2. *J. Phys. Chem. C* **2010**, *114*, 4961.

(31) Wu, Z.; Jiang, B.; Liu, Y. Effect of Transition Metals Addition on the Catalyst of Manganese/Titania for Low-Temperature Selective Catalytic Reduction of Nitric Oxide with Ammonia. *Appl. Catal., B* **2008**, *79*, 347.

(32) Yang, S.; Li, J.; Wang, C.; Chen, J.; Ma, L.; Chang, H.; Chen, L.; peng, Y.; Yan, N. Fe−Ti Spinel for the Selective Catalytic Reduction of NO with NH_3: Mechanism and Structure−Activity Relationship. *Appl. Catal., B* **2012**, *117−118*, 73.

(33) Ma, L.; Li, J.; Ke, R.; Fu, L. Catalytic Performance, Characterization, and Mechanism Study of $Fe_2(SO_4)_3$/TiO_2 Catalyst for Selective Catalytic Reduction of NOx by Ammonia. *J. Phys. Chem. C* **2011**, *115*, 7603.

(34) Apostolescu, N.; Geiger, B.; Hizbullah, K.; Jan, M.; Kureti, S.; Reichert, D.; Schott, F.; Weisweiler, W. Selective Catalytic Reduction of Nitrogen Oxides by Ammonia on Iron Oxide Catalysts. *Appl. Catal., B* **2006**, *62*, 104.

(35) Yang, S.; Wang, C.; Chen, J.; Peng, Y.; Ma, L.; Chang, H.; Chen, L.; Liu, C.; Xu, J.; Li, J.; Yan, N. A Novel Magnetic Fe−Ti−V Spinel Catalyst for the Selective Catalytic Reduction of NO with NH_3 in a Broad Temperature Range. *Catal. Sci. Technol.* **2012**, *2*, 915.

(36) Liu, F.; He, H.; Lian, Z.; Shan, W.; Xie, L.; Asakura, K.; Yang, W.; Deng, H. Highly Dispersed Iron Vanadate Catalyst Supported on TiO_2 for the Selective Catalytic Reduction of NOx with NH_3. *J. Catal.* **2013**, *307*, 340.

(37) Lázaro, M. J.; Boyano, A.; Herrera, C.; Larrubia, M. A.; Alemany, L. J.; Moliner, R. Vanadium Loaded Carbon-Based Monoliths for the on-Board NO Reduction: Influence of Vanadia and Tungsten Loadings. *Chem. Eng. J.* **2009**, *155*, 68.

(38) García-Bordejé, E.; Monzón, A.; Lázaro, M. J.; Moliner, R. Promotion by a Second Metal or SO_2 over Vanadium Supported on Mesoporous Carbon-Coated Monoliths for the SCR of NO at Low Temperature. *Catal. Today* **2005**, *102−103*, 177.

(39) Zhu, Z.; Liu, Z.; Liu, S.; Niu, H. Catalytic NO Reduction with Ammonia at Low Temperatures on V_2O_5/AC Catalysts: Effect of Metal Oxides Addition and SO_2. *Appl. Catal., B* **2001**, *30*, 267.

(40) Teng, H.; Hsu, L.-Y.; Lai, Y.-C. Catalytic Reduction of NO with NH_3 over Carbons Impregnated with Cu and Fe. *Environ. Sci. Technol.* **2001**, *35*, 2369.

(41) Marbán, G.; Fuertes, A. B. Kinetics of the Low Temperature Selective Catalytic Reduction of NO with NH_3 over Activated Carbon Fibre Composite-Supported Iron oxides. *Catal. Lett.* **2002**, *84*, 13.

(42) García-Bordejé, E.; Calvillo, L.; Lázaro, M. J.; Moliner, R. Vanadium Supported on Carbon-Coated Monoliths for the SCR of NO at Low Temperature: Effect of Pore Structure. *Appl. Catal., B* **2004**, *50*, 235.

(43) Xiao, Y.; Liu, Q.; Liu, Z.; Huang, Z.; Guo, Y.; Yang, J. Roles of Lattice Oxygen in V_2O_5 and Activated Coke in SO_2 Removal over Coke-Supported V_2O_5 Catalysts. *Appl. Catal., B* **2008**, *82*, 114.

(44) Dunn, J. P.; Koppula, P. R.; Stenger, H. G.; Wachs, I. E. Oxidation of Sulfur Dioxide to Sulfur Trioxide over Supported Vanadia Catalysts. *Appl. Catal., B* **1998**, *19*, 103.

(45) Huang, Z.; Zhu, Z.; Liu, Z. Combined Effect of H_2O and SO_2 on V_2O_5/AC Catalysts for NO Reduction with Ammonia at Lower Temperatures. *Appl. Catal., B* **2002**, *39*, 361.

(46) García-Bordejé, E.; Pinilla, J. L.; Lázaro, M. J.; Moliner, R. NH_3-SCR of NO at Low Temperatures over Sulphated Vanadia on Carbon-coated Monoliths: Effect of H_2O and SO_2 Traces in the Gas Feed. *Appl. Catal., B* **2006**, *66*, 281.

(47) Boyano, A.; Gálvez, M. E.; Moliner, R.; Lázaro, M. J. Carbon-based Catalytic Briquettes for the Reduction of NO: Effect of H_2SO_4 and HNO_3 Carbon Support Treatment. *Fuel* **2008**, *87*, 2058.

(48) Gálvez, M. E.; Boyano, A.; Moliner, R.; Lázaro, M. J. Low-cost Carbon-based Briquettes for the Reduction of NO Emissions: Optimal Preparation Procedure and Influence in Operating Conditions. *J. Anal. Appl. Pyrolysis* **2010**, *88*, 80.

(49) Gao, X.; Liu, S.; Zhang, Y.; Luo, Z.; Cen, K. Physicochemical Properties of Metal-doped Activated Carbons and Relationship with Their Performance in the Removal of SO_2 and NO. *J. Hazard. Mater.* **2011**, *188*, 58.

(50) Bai, S.; Zhao, J.; Wang, L.; Zhu, Z. SO_2-Promoted Reduction of NO with NH_3 over Vanadium Molecularly Anchored on the Surface of Carbon Nanotubes. *Catal. Today* **2010**, *158*, 393.

(51) Liu, Q.; Liu, Z.; Wu, W. Effect of V_2O_5 Additive on Simultaneous SO_2 and NO Removal from Flue Gas over a Monolithic Cordierite-based CuO/Al_2O_3 Catalyst. *Catal. Today* **2009**, *147*, S285.

(52) Ma, J.; Liu, Z.; Liu, S.; Zhu, Z. A Regenerable Fe/AC Desulfurizer for SO_2 Adsorption at Low Temperatures. *Appl. Catal., B* **2003**, *45*, 301.

(53) Li, P.; Liu, Q.; Liu, Z. Behaviors of NH_4HSO_4 in SCR of NO by NH_3 over Different Cokes. *Chem. Eng. J.* **2012**, *181−182*, 169.

(54) Roy, S.; Viswanath, B.; Hegde, M. S.; Madras, G. Low-Temperature Selective Catalytic Reduction of NO with NH_3 over $Ti_{0.9}M_{0.1}O_{2-\delta}$ (M = Cr, Mn, Fe, Co, Cu). *J. Phys. Chem. C* **2008**, *112*, 6002.

(55) García-Bordejé, E.; Pinilla, J. L.; Lázaro, M.; Moliner, R.; Fierro, J. L. G. Role of Sulphates on the Mechanism of NH_3-SCR of NO at Low Temperatures over Presulphated Vanadium Supported on Carbon-Coated Monoliths. *J. Catal.* **2005**, *233*, 166.

(56) Liu, F.; Asakura, K.; He, H.; Shan, W.; Shi, X.; Zhang, C. Influence of Sulfation on Iron Titanate Catalyst for the Selective Catalytic Reduction of NOx with NH_3. *Appl. Catal., B* **2011**, *103*, 369.